Chemistry & Biology
Article

Design of Peptide Inhibitors for the Importin α/β Nuclear Import Pathway by Activity-Based Profiling

Shunichi Kosugi,[1,2,3,*] Masako Hasebe,[1] Tetsuyuki Entani,[3] Seiji Takayama,[3] Masaru Tomita,[1] and Hiroshi Yanagawa[1,2,*]
[1]Institute for Advanced Biosciences, Keio University, Tsuruoka 997-0017, Japan
[2]Department of Biosciences and Informatics, Faculty of Science and Technology, Keio University, Yokohama 223-8522, Japan
[3]Graduate School of Biological Sciences, Nara Institute of Science and Technology, Ikoma 630-0192, Japan
*Correspondence: skosugi@bs.naist.jp (S.K.), hyana@bio.keio.ac.jp (H.Y.)
DOI 10.1016/j.chembiol.2008.07.019

SUMMARY

Despite the current availability of selective inhibitors for the classical nuclear export pathway, no inhibitor for the classical nuclear import pathway has been developed. Here we describe the development of specific inhibitors for the importin α/β pathway using a novel method of peptide inhibitor design. An activity-based profile was created via systematic mutational analysis of a peptide template of a nuclear localization signal. An additivity-based design using the activity-based profile generated two peptides with affinities for importin α that were approximately 5 million times higher than that of the starting template sequence. The high affinity of these peptides resulted in specific inhibition of the importin α/β pathway. These peptide inhibitors provide a useful tool for studying nuclear import events. Moreover, our inhibitor design method should enable the development of potent inhibitors from a peptide seed.

INTRODUCTION

Active import of proteins in the nucleus is primarily determined by the interaction of nuclear localization signals (NLSs) contained in cargo proteins and with specific NLS receptors, including the importin α and importin β families (Görlich et al., 1995; Jans et al., 2000). Importin α, the main NLS receptor, relieves its autoinhibition (established through intramolecular interaction through the N-terminal importin β-binding (IBB) domain) by interacting with importin β1; this enables high-affinity binding of importin α to an NLS within a cargo. The importin α/β-cargo complex enters the nucleus and is dissociated by the binding of Ran-GTP to importin β1, which induces recycling of the importins to the cytoplasm (Görlich and Kutay, 1999; Weis, 2003). The nuclear pore protein Nup2p and the importin α-export complex Cse1p-Ran-GTP also contribute to the importin α-cargo dissociation (Gilchrist et al., 2002; Gilchrist and Rexach, 2003; Hood et al., 2000; Hood and Silver, 1998; Solsbacher et al., 2000). In addition to the importin α/β pathway, it is known that there are at least 10 importin β-dependent nuclear import/export pathways. Importin α-independent pathways mediate the nuclear import of a number of specific proteins, the NLSs of which are directly recognized by several importin β members, including importin β1 and importin β2 (transportin) (Harel and Forbes, 2004).

Importin α recognizes two classes of NLS, termed the classical NLSs, which are either monopartite (with a single cluster of basic amino acid residues) or bipartite (with two clusters of basic amino acids separated by a 10–12 aa linker) (Lange et al., 2007). The SV40 large T antigen NLS (PKKKRKV) and nucleoplasmin NLS (KRPAATKKAGQAKKKK) have often been cited as prototypes of monopartite and bipartite NLSs, respectively. The monopartite NLS has been defined as a sequence composed of at least four consecutive basic amino acids or represented by a putative consensus sequence, K(K/R)X(K/R), where *X* indicates any amino acid. A putative consensus sequence of the bipartite NLS has been defined as (K/R)(K/R)X10–12(K/R)3/5, where (K/R)3/5 represents a region in which at least three of five consecutive amino acids are either lysine or arginine, and in which the linker region has been found to be tolerant to amino acid conversion (Robbins et al., 1991). Despite these definitions of minimum consensus patterns, a strict consensus has yet to be established because of sequence diversity.

Nuclear export of proteins is mediated mainly by an importin β member, termed CRM1 or exportin, which recognizes nuclear export signals (NESs) contained in cargo proteins (Weis, 2003). Leptomycin B, an antifungal antibiotic from a Streptomyces strain, targets CRM1 and specifically inhibits the CRM1-dependent nuclear export pathway (Yashiroda and Yoshida, 2003). This inhibitor has been used as a reagent in studying for nuclear export activities or NESs. In the case of nuclear import, there is currently no general inhibitor available, although a cell-permeable peptide containing an NF-κB NLS has been developed as an inhibitor for the nuclear import of a subset of stress-responsive transcription factors, including NF-κB, AP-1, NFAT, and STAT1, and this has often been used as an inhibitor of NF-κB (Lin et al., 1995; Torgerson et al., 1998). Recently, a nuclear import inhibitor specific to the transportin-dependent pathway has been developed by a structure-based design (Cansizoglu et al., 2007).

Because peptide inhibitors can cover large interface areas that are required for protein-protein interaction, they have a potential to interact with targets more strongly than small molecule inhibitors. Two current strategies for developing peptide inhibitors are as follows: (i) those based on directed evolution involving high-throughput library screening, and (ii) rational design involving the use of sequence and structural information regarding protein-protein interfaces (Privé and Melnick, 2006; Sato et al., 2006). These strategies, however, are often unsuccessful in generating specific, high-affinity peptide binders because the

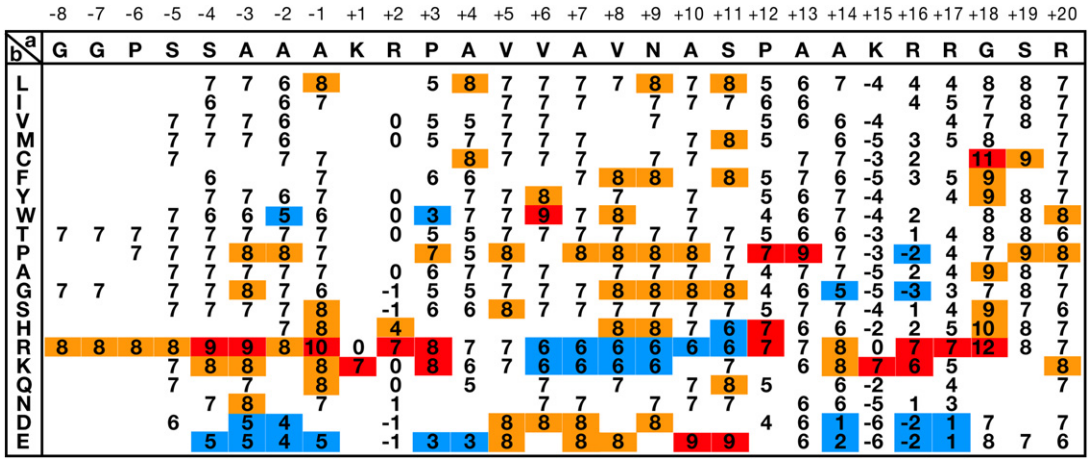

Figure 1. Activity-Based Profile of a Classical Bipartite NLS

A single amino acid residue within the template sequence indicated in the top line in the matrix was replaced with various other residues indicated in the left column, and the nuclear import activity was assayed in budding yeast. Activity scores were determined as in Figure S1. At several mutational positions, modified templates with different levels of basal activity were used to obtain scores less than 1 and greater than 10. Blanks represent undetermined scores. Scores with higher, slightly higher, and lower activities than an average value for each position are shown in red, orange, and blue, respectively.

directional evolution often results in isolation of nonspecific binders and involves trial-and-error experiments. The rational design also requires structural information of target proteins and theoretical framework for designing inhibitors. The disadvantage of these strategies necessitates the development of more effective strategies for obtaining specific, potent peptide inhibitors.

In this study, we present a strategy for designing potent peptide inhibitors. The strategy optimizes peptide sequences by selecting the residues with the highest activity scores that are represented in an activity-based peptide profile. Using a profile generated from an NLS template sequence, we developed the first nuclear import inhibitors that are specific for the importin α/β pathway.

RESULTS

Activity-Based Profiling of a Bipartite NLS Highlights Position-Dependent Activating and Repressing Residues

To determine the patterns and amino acid residues responsible for nuclear import activity of an importin α-dependent classical NLS, we conducted a systematic amino acid replacement analysis for a bipartite NLS, which can yield a potentially stronger activity than the monopartite NLS (Hodel et al., 2001). We used an artificial bipartite NLS as a template, comprising 28 amino acids that contain the minimum consensus and that exhibit a moderate level of activity in budding yeast and mammalian cells. We systematically replaced the residue at each position with as many other amino acids as possible. Mutated sequences were analyzed for nuclear import activity with a reporter of β-glucuronidase (GUS) fused with green fluorescent protein (GFP) in yeast; their activities were scored on a 10-point scale based on the extent of nuclear localization (see Figure S1 available online). Overall findings are represented in a score matrix showing an activity-based NLS profile (Figure 1). The profile revealed previously unrecognized features of bipartite NLSs and highlighted a number of specific residues that activate or repress the overall activity of the NLS in a position-dependent manner. Though basic and acidic residues were activators and repressors, respectively, in the regions adjacent to the core basic stretches, this was reversed (i.e., basic residues were repressors, acidic residues activators) in the central linker region (Figure 1 and Figure S2). Within the N- and C-terminal basic regions, a specific basic pattern and residue were required for activity. Activating and repressing residues were present in more extended regions toward the N and C termini than has previously been reported (Robbins et al., 1991). Similar residue-specific and position-dependent effects were observed for other NLS templates (Figures S2 and S3). These findings indicate that various amino acids have position-specific effects on activity throughout the entire NLS region, in contrast with previous observations and the minimum consensus of bipartite NLSs (Robbins et al., 1991).

Peptide Sequences bimax1 and bimax2, Designed Using the NLS Profile, Bind Tightly to Full-Length Importin Alphas

Simultaneous amino acid replacement at two positions within NLSs revealed that the contribution of each residue to the overall activity was in most cases independent and additive (Figure S3). Thus, it is expected that NLS variants with the highest activities can be designed by selecting the amino acids with the highest scores at each position in the NLS profile. We designed two putative inhibitor sequences (bimax1 and bimax2), each with an optimal summed score but differing at nine positions (Figure 2A). Both sequences bound tightly to the full-length yeast importin α Kap60p (Figure 2C), in contrast with SV40 monopartite and nucleoplasmin (NP) bipartite NLSs, which bound only to Kap60p-ΔIBB, a variant lacking the autoinhibitory domain (Figure 2B). Furthermore, these peptides bound tightly to full-length versions of four mammalian importin α members (importins α1, α3, α6, and α7, representatives of three subclasses of the mammalian importin α family), but did not bind to importin β1 (Figure 2D), whereas

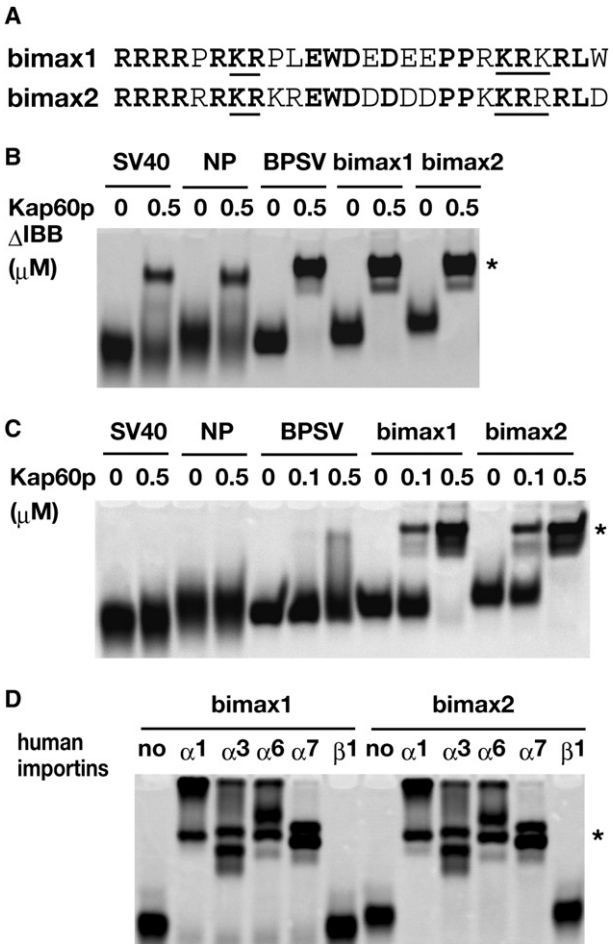

Figure 2. Importin α-Binding Properties of Peptide Inhibitors Designed Using the NLS Profile

(A) Two peptide sequences optimized from the NLS profile. Two peptide sequences, bimax1 and bimax2, were designed by selecting residues with the highest scores at each position, as represented in the NLS profile. Regions corresponding to the N- and C-terminal basic stretches of the template NLS are underlined.

(B) Binding assays for NLS variants and Kap60pΔIBB. Thioredoxin (Trx)-GFP fusions with SV40 NLS (SV40), nucleoplasmin NLS (NP), BPSV40 NLS (BPSV), bimax1, and bimax2 (0.5 μM each) were incubated with Kap60pΔIBB fused with glutathione S-transferase (GST) in the indicated concentrations, and the bound complexes were separated by native PAGE. GFP-NLS-Kap60pΔIBB complexes are indicated by an asterisk.

(C) Binding assays for NLS variants and the full-length Kap60p. In vitro binding assays were carried out with the indicated GFP-NLS variants (0.5 μM) and full-length Kap60p fused with GST in the indicated concentrations, as in (B).

(D) Binding assays for bimax1 and bimax2 and full-length mammalian importin α members. The binding assays were carried out with GFP-bimax1 or GFP-bimax2 (0.5 μM) and full-length importin α or importin β1 fused with GST (0.5 μM), as in (B).

SV40NLS did not bind to any of these importins (data not shown). These findings indicate that both bimax1 and bimax2 are strong and specific binders for the importin α family.

To determine the equilibrium dissociation constants (K_d) of bimax1 and bimax2 for binding to importin α, surface plasmon resonance (SPR) analyses were performed using a Biacore system. NLS peptide variants fused with Trx-GFP were directly immobilized on the sensor chip surfaces by thiol coupling. Various concentrations of analytes (i.e., GST-Kap60p and GST-Kap60pΔIBB) were injected into peptide-immobilized flow cells to obtain SPR sensorgrams (Figure 3). During injection of analytes to reference cells on which Trx-GFP alone was immobilized, no nonspecific binding was observed. The K_d values for these interactions were determined through a nonlinear regression fitting to a Langmuir binding model using BIAevaluation software (Table 1). The K_d of SV40NLS for binding to Kap60pΔIBB was approximately 5 nM, which correlated roughly with those reported previously, whereas the K_d values of BPSV40 NLS were about one order of magnitude higher than previously reported values (Hodel et al., 2001). Although this difference is possibly due to a different construction of BPSV40 NLS or different experimental conditions between the studies, the difference (197-fold) between the K_d values of BPSV40 for binding to Kap60p and Kap60pΔIBB correlated roughly with those (120-fold) reported previously (Hodel et al., 2001). Thus, the K_d values of bimax peptides for binding to Kap60pΔIBB was estimated by dividing the K_d values (480 pM for bimax 1 and 4.4 pM for bimax 2) for the full-length Kap60p by 197, as they were too low to be determined directly (Table 1). Consequently, the estimated K_d values of bimax1 and bimax 2 for Kap60pΔIBB was approximately 2.4 pM and 0.02 pM, respectively—the latter value being 4.8 million times lower than that of the starting NLS template ($NLS_{score\ 7}$) (Table 1). The potential dimerization ability of GST (K_d = 0.34 mM) (Vargo et al., 2004) may lead to a higher apparent affinity because of avidity effect. The avidity effect occurs through a simultaneous binding of a dimer of GST fusion proteins to two adjacent ligand molecules, resulting from a dense immobilization of a ligand on a solid surface (Ladbury et al., 1995). However, it is most likely that the GST-Kap60p and GST-Kap60pΔIBB fusion proteins bind to the immobilized ligands in monomer because of low densities (9–18 fmol mm^{-2}) of our ligands (Trx-GFP-NLS fusion proteins) immobilized on sensor chip surfaces and relatively low concentrations of analytes (GST-Kap60p fusion proteins) applied to the sensor chips. The low concentrations of ligands and analytes also resulted in little influence by mass transfer limitation (analyte rebinding). Thus, these findings show that both bimax peptide sequences have extremely high affinities for importin α and that a strong peptide binder can be designed using the activity-based peptide profile.

Both bimax1 and bimax2 Severely Inhibit Cell Growth and Importin α-Mediated Nuclear Import in Yeast

Because the importin α/β pathway is the major activity for protein nuclear import, blocking this pathway should inhibit cell growth. We tested whether bimax1 and bimax2 inhibit the growth of yeast. Expression of these sequences fused to GFP severely inhibited the growth of yeast, even when a low-copy plasmid was used; BPSV40 had no effect on growth (Figure 4A), as was also shown in a previous study (Hodel et al., 2006). This observation suggests that both peptide sequences, even at low concentrations, bind tightly to Kap60p in vivo to block the importin α/β pathway. In mammalian cells, transfection of bimax expression plasmids appeared to cause growth inhibition of the cells and cell death in a portion of the cells (data not shown), although it is not clear whether this cell death results from growth inhibition or apoptosis.

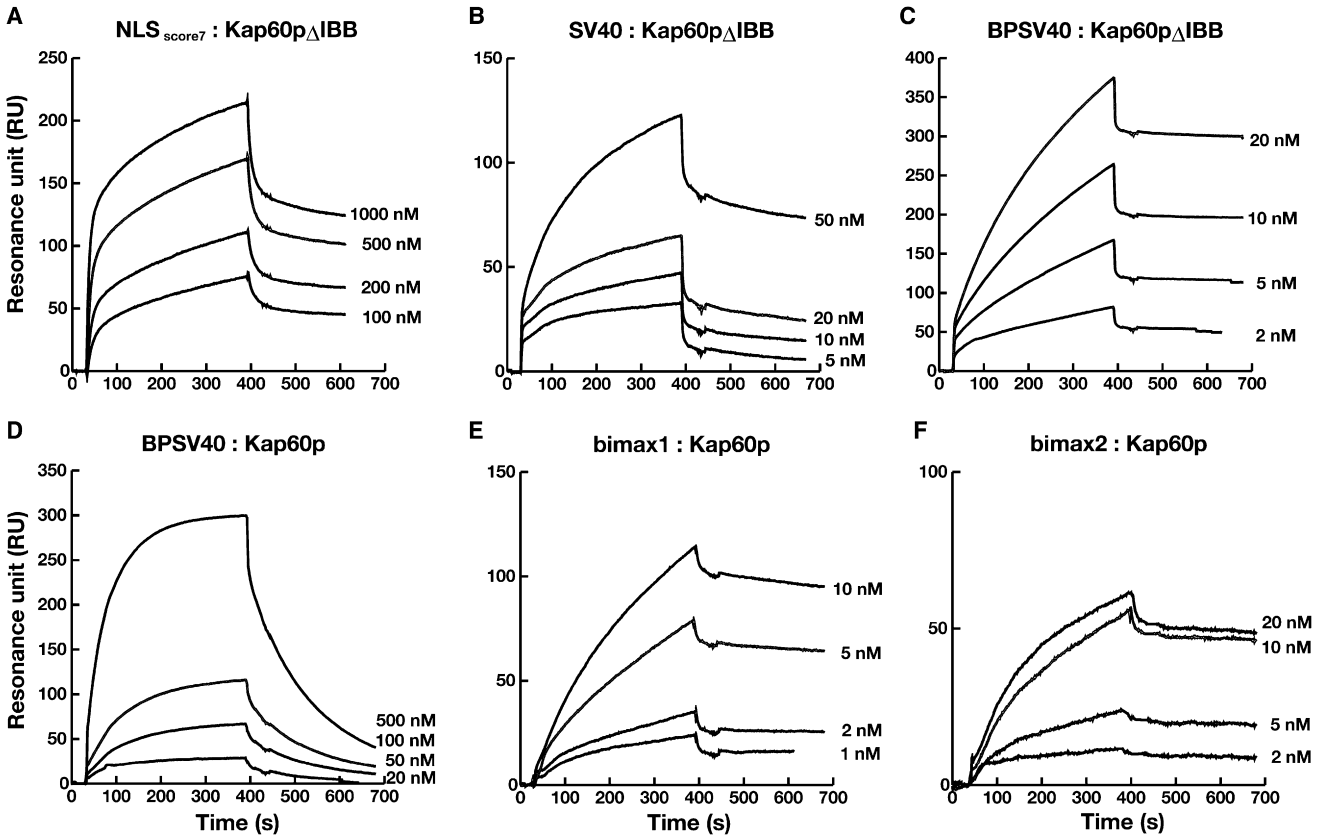

Figure 3. SPR Analysis of the Interactions between Importin α and NLS Variants

Trx-GFP fused with $NLS_{score\ 7}$ (A), SV40 NLS (B), BPSV40 NLS (C and D), bimax1 (E), and bimax2 (F) were immobilized on Biacore sensor chips by thiol coupling. $NLS_{score\ 7}$ is the template NLS with activity score of 7, which was used for the generation of the NLS profile. The indicated concentrations of Kap60pΔIBB (A–C) and Kap60p (D–F) were injected into flow cells of the sensor chips in 60 μl injection volumes and at a flow rate of 10 μl min^{-1}.

We next examined whether bimax1 and bimax2 inhibit nuclear import activity in yeast. Inducible expression of bimax1 and bimax2 using the *GAL1* promoter from pYES-Grx1-NLS plasmids significantly inhibited the nuclear localization of GUS-GFP fused with the SV40 NLS and nucleoplasmin bipartite NLS, but had only a minor effect on the NLS of Nab2p, a poly(A) RNA binding protein, in which transport activity is mediated by Kap104p (transportin) (Siomi et al., 1998; Truant et al., 1998; Figure 4B). These findings suggest that bimax1 and bimax2 are potent and selective inhibitors of the importin α/β pathway.

Both bimax1 and bimax2 Specifically Inhibit Nuclear Import Activity Mediated by the Importin α/β Pathway in Mammalian Cells

We examined whether the specific inhibitory effects of bimax1 and bimax2 also occur in mammalian cells, in which multiple importin α members are present. Coexpressions of bimax1 or bimax2 with GUS-GFP-NLS reporters specifically inhibited the importin α-mediated nuclear import pathway (SV40 and NP NLSs) but not the importin β1-mediated pathway (Snail and SREBP-2, a zinc finger transcription factor and sterol regulatory element-binding transcription factor 2, respectively) (Nagoshi et al., 1999; Yamasaki et al., 2005), the transportin-mediated pathway (hnRNP A1) (Pollard et al., 1996), or the importin-7-mediated pathway (EZI, a zinc finger protein) (Saijou et al., 2007; Figure 5A). These findings indicate that the bimax1 and bimax2 inhibitors are specific to the importin α/β pathway and are likely to be effective for multiple members of importin α in mammalian cells.

Importin α-Dependent Noncanonical NLSs of p107 and PIASy Determined Using Bimax Inhibitors

We also tested the effects of the inhibitors on the localization of two nuclear proteins p107, a retinoblastoma-associated protein, and PIASy, a SUMO E3 ligase, for which nuclear import receptors are unknown. When these proteins, fused with GFP, were coexpressed with either of the peptide inhibitors, their localization to the nucleus was significantly inhibited (Figure 5), suggesting that this localization is dependent on the importin α/β pathway. This result further suggests that these two proteins have classical NLSs bearing the consensus basic stretches. The p107 protein (1-1063), however, contains no potential NLS matching the minimum consensus patterns of the classical NLSs; it does however contain a bipartite NLS-like sequence (p107-NLS, 1021-QKTKKRVIAISGDADSPAKRLCQE) at the C terminus. PIASy (1-510) contains a putative monopartite NLS (PIASy-NLS1, 52-PELFKKIKELYE) matching the monopartite consensus pattern in the N-terminal region, whereas there exists a non-canonical monopartite NLS-like sequence (PIASy-NLS2,

Table 1. Dissociation Constants for the Interaction between Importin α and NLS Variants

NLS	Importin α	K_d (nM)
$NLS_{score\ 7}$	Kap60pΔIBB	96 ± 9
SV40	Kap60pΔIBB	4.8 ± 0.2
BPSV40	Kap60pΔIBB	0.34 ± 0.1
BPSV40	Kap60p	67 ± 15
bimax1	Kap60p	0.48 ± 0.17
bimax2	Kap60p	0.0044 ± 0.0009
bimax1	Kap60pΔIBB	(0.0024)[a]
bimax2	Kap60pΔIBB	(0.00002)[a]

The sensorgrams shown in Figure 3 were fitted to 1:1 Langmuir model using BIAevaluation 3.1 software to determine dissociation equilibrium constants (K_d). The averages of the values obtained for four different concentrations of importin α and the standard errors are given for the indicated interactions.

[a] Values estimated from the K_d values of bimax 1/2 for binding to Kap60p. These K_d values were divided by 197 K_d, which is the difference in K_d between the full-length and truncated Kap60p, calculated from the K_d values of BPSV40.

494-PRPKRRCPFQK) at the C terminus. The deletion of the C terminus from either of these proteins (p107ΔC and PIASyΔC) led to a significant loss in nuclear import activity (Figure 5B), suggesting that p107-NLS and PIASy-NLS2 play a major role in the nuclear import of these two proteins. GUS-GFP fusions with p107-NLS and PIASy-NLS2 were localized to the nucleus, and their nuclear localizations were effectively inhibited by coexpression with bimax2, whereas PIASy-NLS1 exhibited no considerable nuclear import activity (Figure 5B). These findings indicate that the importin α-mediated nuclear localizations of p107 and PIASy are directed by p107-NLS and PIASy-NLS2, respectively, but not by NLSs with known consensus patterns. Moreover, the fact that neither the deletion of these NLSs nor the inhibition by bimax2 expression completely removed the nuclear import activities of these proteins suggests that pathways other than the importin α/β pathway make a partial contribution to their nuclear import.

Importin α-Inhibitor Complex Is Resistant to Cargo Release Activities in the Nucleus

The in vitro and in vivo analyses described previously suggest that the observed nuclear import inhibition by bimax1 and bimax2 is due to an importin β1-independent interaction of the inhibitors with importin α, which circumvents the cargo release process mediated by interaction of importin β1 and Ran-GTP. There remains the possibility that the importin α-inhibitor complex is dissociated by another cargo release factor, such as Nup2p or Cse1p-Ran-GTP. We examined whether Kap60p stably forms a complex with the inhibitor in vivo. We constructed a yeast strain (*KAP60-GFP*) in which a Kap60p-HA-GFP fusion protein was expressed under the control of its own promoter at the native chromosomal locus. The strain was transformed with pYES-Grx1-NLS-FLAG constructs, and interaction of Kap60p-HA-GFP with the induced NLS variants was analyzed by immunoprecipitation. Western blotting showed that the expression of Grx1-bimax2-Flag was considerably lower than that of other Grx1 fusions (Figure 6A), indicating a cell toxic effect of bimax2. Nevertheless, only Grx1-bimax2-Flag was coimmunoprecipitated with a significant amount of Kap60p-HA-GFP (Figure 6A). This result confirms that the bimax inhibitors form a stable complex with importin α independently of importin β1 in vivo.

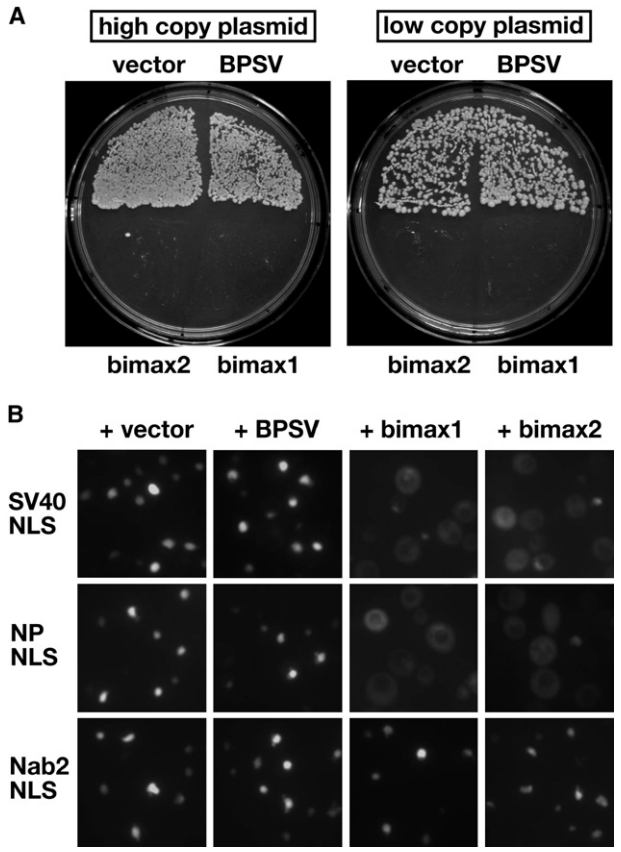

Figure 4. Expression of bimax1 and bimax2 Peptides in Budding Yeast

(A) Growth inhibition of yeast by bimax peptide expression. Yeast was transformed with high-copy plasmids (pGAD-GFP) or low-copy plasmids (pAUA-GFP), encoding the indicated peptide sequences (BPSV40 NLS, bimax1, and bimax2) to express their GFP fusions. Transformed cells were plated on a quarter of SD plates lacking leucine or uracil, and cultured for 3 days at 30°C.

(B) Inhibition assay for nuclear import activity in yeast. GUS-GFP fused with the NLSs indicated in the left column and a yeast protein Grx1p fused with the NLSs indicated in the top line were simultaneously expressed using galactose-inducible vectors (pYES-GFP3 and pYES-Grx1). GFP fluorescence was observed 2 hr after galactose induction.

It is known that ablation of the cargo release machinery leads to nuclear accumulation of importin α (Gilchrist and Rexach, 2003; Harreman et al., 2003; Hood et al., 2000; Hood and Silver, 1998; Solsbacher et al., 2000). We examined whether the subcellular localization of Kap60p is affected by inhibitor expression. Prior to expression, Kap60p-GFP was localized throughout the cell with some accumulation in the nucleus. This localization pattern was altered to one of intensive nuclear localization by expression of Grx1-bimax2, whereas no significant change was observed as a result of expression of the SV40 or BPSV40 NLS fusion (Figure 6B). Similar localization changes were observed in mammalian cells. Importins α1, α3, and α7 fused with GFP were partially nuclear, though it has been reported that endogenous importin alphas are more evenly distributed throughout the

A

GFP fusions	reported receptor importin	nuclear localization (%) competitor vector	SV40	BPSV	bimax1	bimax2
SV40	α/β	97	99	99	10	2
NP	α/β	98	99	98	4	1
Snail	β1	80	88	88	85	82
SREBP	β1	98	96	98	97	97
hnRNP	β2	100	100	100	100	100
EZI	7	100	100	100	99	100
p107	unknown	100	100	90	3	4
PIASy	unknown	100	100	100	0	0

B

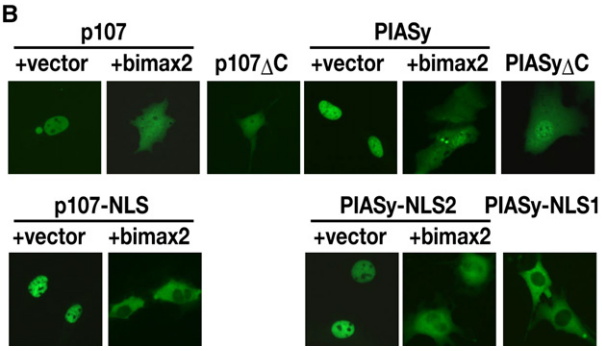

Figure 5. Specific Inhibition of the Importin α/β Pathway by bimax1 and bimax2 in Mammalian Cells

(A) Inhibition assay for nuclear import activity in mammalian cells. Cotransfection into NIH 3T3 cells was conducted using reporter plasmids (pCMV-GFP2 or pCMV-GFP3) encoding GFP or GUS-GFP fused with the NLSs or proteins (as indicated in the left column) and competitor expression plasmids (pCMV-Grx1) encoding Grx1p fused with the NLSs (as indicated in the second line). The number of cells exhibiting nuclear localization of the GFP reporters was recorded as a percentage of the total GFP-positive cells, whereas cells exhibiting localization to both the nucleus and cytoplasm were not counted as nuclear localized cells.

(B) Identification of NLSs responsible for the nuclear import of PIASy and p107. Reporter plasmids encoding GFP fused with PIASy or p107 were cotransfected with the bimax2 competitor expression plasmid. Reporter plasmids encoding GFP fused with the C-terminal truncated versions of PIASy and p107 (PIASyΔC [1–493] and p107ΔC [1–1020], respectively) were transfected into NIH 3T3 cells. Reporter plasmids encoding GUS-GFP fused with p107-NLS, PIASy-NLS1 or PIASy-NLS2 were cotransfected with the bimax2 competitor expression plasmid.

A

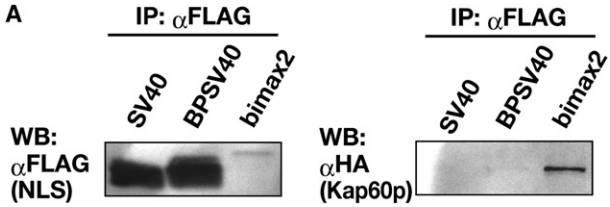

B

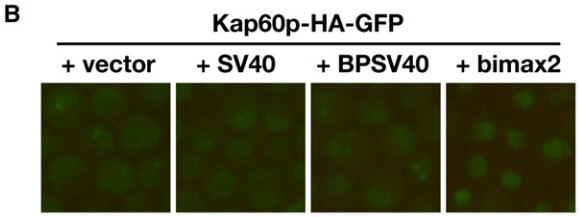

C

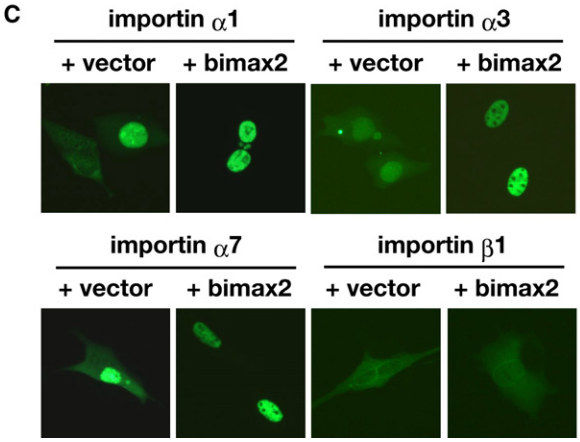

Figure 6. Resistance of Importin α-bimax Inhibitor Complex to Cargo Release Activities

(A) Kap60p-bimax2 complex detected by immunoprecipitation. pYES-Grx1-FLAG plasmids encoding the indicated NLSs (SV40, BPSV40, and bimax2) were introduced into a *KAP60-GFP* strain, which expresses Kap60p fused with a hemagglutinin (HA)-GFP tag. Grx1-NLS-FLAG fusion proteins were induced with galactose for 3 hr in yeast in a log phase. Proteins immunoprecipitated with anti-FLAG agarose were subjected to western blotting with antibodies against the FLAG and HA tags.

(B) Increased nuclear accumulation of Kap60p by bimax2. The indicated Grx1-NLS-FLAG fusion proteins were induced in the *KAP60-GFP* strain, as in (A).

(C) Increased nuclear accumulation of importin alphas by bimax2 in mammalian cells. Plasmids (pCMV-GFP2) encoding GFP fusion proteins with importins α1, α3, α7, and β1 were cotransfected with the competitor expression plasmids encoding bimax2 into NIH 3T3 cells. Photos are representatives of the observed GFP localization patterns; for GFP-importin α1, most cells exhibiting nonnuclear phenotypes of GFP (35% of the total GFP-positive cells) were changed to cells with a nuclear phenotype by coexpression of bimax2.

cells (Miyamoto et al., 2002). Nevertheless, these proteins were localized completely to the nucleus on coexpression with bimax2; the localization of importin β1 was unaffected by bimax2 (Figure 6C). These findings suggest that the bimax inhibitors antagonize cargo release activities to restrict importin α recycling and deplete a pool of free importin α.

DISCUSSION

'The peptide inhibitors bimax1 and bimax2 efficiently block nuclear import activity mediated by the importin α/β pathway. The high affinity of these inhibitors for importin α (K_ds in the picomolar range) allows importin β1-independent binding to importin α and prevents the importin α-inhibitor complex from the dissociation that would normally occur, allosterically modulated by cargo release factors, including importin β1 and Ran-GTP. Although BPSV40 NLS is able to bind importin α independently of importin β1, it cannot inhibit nuclear import activity. Hence, Nup2p or Cse1p-Ran-GTP may make a major contribution to the dissociation of the BPSV40-importin α complex in the nucleus. Given that the apparent K_d of BPSV40 for the full-length Kap60p is in the low nanomolar range (Hodel et al., 2001), NLS peptides that can

overcome cargo release activities require a K_d for importin α in the high picomolar range. This high-affinity barrier to antagonizing cargo release activity would prevent the occurrence of natural NLSs that can inhibit their own nuclear import pathway.

The high affinity of bimax peptides allows us to observe their inhibitory effect using tranfected plasmids that express fusion proteins containing the peptide inhibitors. In mammalian cells and yeast, in vitro nuclear transport assays can be employed in a reconstitution system with permeabilized semi-intact cells and recombinant importin proteins and/or cytosol (Görlich et al., 1994; Schlenstedt et al., 1993). Although this system is valuable in analyzing the nuclear transport process for a protein, difficulty exists in reconstituting cell environments for different species and cell types, especially for proteins whose nuclear import is regulated by a change in physiology or an artificial condition. The bimax inhibitors, coupled with the plasmid-based expression, would complement or substitute for the reconstitution assays and provide a useful reagent to identify the importin α/β pathway, as shown for p107 and PIASy.

Many currently available peptide inhibitors have been used as reagents with a cell permeable property. An NF-κB NLS-derived cell-permeable peptide (SN50) has been reported to inhibit the nuclear import of NF-κB, AP-1, NFAT, and STAT1 (Lin et al., 1995; Torgerson et al., 1998). The high dosage (75–100 μM) required for effective inhibition (Torgerson et al., 1998) suggests that, unlike bimax inhibitors, SN50 is likely to act as a simple competitive inhibitor for a subset of importin α/β dimers. In addition, recent studies showed that c-Fos and c-Jun, components of AP-1, are not imported to the nucleus through the importin α/β pathway (Arnold et al., 2006; Forwood et al., 2001; Waldmann et al., 2007) and that STAT1 binds to the minor binding site of importin α in contrast with the NF-κB NLS (Fagerlund et al., 2005; Sekimoto et al., 1997). These observations suggest that SN50 may also inhibit nuclear import pathways that do not involve importin α. Thus, the bimax inhibitors could also be used as cell-permeable peptide reagents that are more sensitive and specific to the importin α/β pathway than SN50.

Peptide inhibitors in general are thought to have higher affinities for targets (especially for interfaces involved in protein-protein interaction) than small molecule inhibitors, owing to their potentially larger contact with the targets. It has been found that only a small subset of amino acids at a particular protein interface, termed a hot spot, is responsible for a major binding affinity, suggesting that large molecules are not necessary for hot spot targeting (Neduva and Russell, 2006; Wells and McClendon, 2007). The findings of the present study suggest that residues with a minor role in interaction are also important in developing a high affinity binder. The hot spot for importin α-NLS interaction exists in the major and minor binding pockets of importin α, both of which interact with the core basic stretches of traditional NLSs (Conti et al., 1998). The NLS profile generated in this study shows not only a major contribution of the core basic stretches, but also a moderate or minor contribution of the residues in the linker and flanking regions. Additional mutational analyses showed that the contribution of each residue within an NLS to the entire activity is independent and additive. Although the effect of each residue within the non-hot-spot regions is small, the sum of the minor contributions can greatly improve the affinity of peptide binders. This additive contribution may be based on the additivity principle in protein thermodynamics (Mildvan, 2004; Wells, 1990). The additivity rule has been adopted to engineer improved proteins (Fox et al., 2007; Sandberg and Terwilliger, 1993); however, a global design is restricted because additivity occurs only if the residues are independent and apart in the protein structure (Mildvan, 2004; Wells, 1990). Although it is not clear whether the additivity observed for NLS peptides corresponds to the thermodynamics additivity observed for proteins, our observations indicate that the additivity based on activity scale measured by our nuclear import assay can be applied for every residue within NLSs and suggest that the additivity-based design of peptide inhibitors is applicable to other unstructured peptides and protein motifs. The generation of an activity-based profile of a 20 aa peptide could be achieved within 4–6 weeks by a single researcher (or in a shorter period using an automated plasmid isolation machine).

SIGNIFICANCE

Peptide inhibitors that disrupt protein-protein interaction are a good alternative to small-molecule inhibitors because of their higher potency, specificity, and safety for therapeutic use. Two strategies, directed evolution and rational design, have been currently employed in developing peptide inhibitors. These strategies are, however, often unsuccessful in generating high-affinity peptide binders. This study presents a strategy for the development of potent peptide inhibitors without using protein structural information. This method uses an activity-based profile generated for a linear peptide, which represents the functional contribution of various amino acids substituted at each position within a template peptide sequence. Optimal peptides can be designed by selecting amino acids with the highest contribution at each position from the activity-based profile. Validity of this method has been shown by using an NLS template sequence. The designed peptides (bimax1 and bimax2) bind tightly to importin α independently of importin β, which confers resistance to cargo release activities in the nucleus. Both bimax1 and bimax2 are identified as the first inhibitors that specifically inhibit the classical nuclear import pathway mediated by importin α. Using these inhibitors we have found that the nuclear import of p107 and PIASy is directed by noncanonical NLSs that depend on the importin α/β pathway, showing the utility of these inhibitors for studying cellular signaling events involving nuclear import. This strategy should enable the development of potent inhibitors from a peptide seed with weak or physiological binding activity, and complements traditional directed evolution and rational design approaches.

EXPERIMENTAL PROCEDURES

Plasmid Construction

The genomic coding sequence of yeast importin α (the full-length Kap60p/Srp1p) was PCR amplified with a primer set (Kap60-N and Kap60-C) (Table S1), using yeast (*S. cerevisiae*) genomic DNA as template. A DNA fragment encoding its N-terminally truncated variant (Kap60pΔIBB) was generated by PCR with a primer set (Kap60Δ-N and Kap60-C) to preclude the N-terminal region (residues 1–71) corresponding to the IBB domain. The PCR fragments were digested with restriction enzymes, whose sites were included in the primer

sequences, and cloned into the corresponding sites of pGEX-6P-1 (Amersham Biosciences, GE Healthcare; Tokyo, Japan). The cDNA sequences of the full-length human importins α1 (accession number CAC83080), α3 (AAH34493), α6 (AAH47409), α7 (AAC15233), and β1 (AAH36703) were PCR amplified with primers (Table S1) using oligo(dT)-primed first-strand cDNAs from human fetal brain (Nippon Gene; Toyama, Japan) for importin α3 and human full-length cDNA clones (Toyobo; Osaka, Japan) for the others. The amplified fragments were cloned into the corresponding sites of pGEX-6P-1 or pGEX-8P, a multicloning site (MCS)-modified version of pGEX-6P-1. For thioredoxin (Trx)-GFP fusions, the GFP coding region derived from an enhanced GFP expression vector pQBI25-fC1 (Qbiogene; Carlsbad, CA) was amplified with a primer set (GFP-N and GFP-C), digested with *Nco*I and *Xho*I, and inserted into the corresponding site of a modified pET-32a (Novagen, Merck; Darmstadt, Germany), in which the *Xba*I site in pET-32a had been precluded, to generate pET-GFP. Double-stranded oligonucleotides encoding NLS peptides, including SV40, nucleoplasmin (NP), BPSV40, bimax1, and bimax2 (Table S1), were inserted into the *Xba*I and *BamHI* sites of pET-GFP to generate plasmids encoding Trx-GFP-NLS fusion proteins. In a similar way, plasmids encoding GST-NLS fusion proteins, which were used for a competition binding analysis, were generated by inserting the same oligonucleotides into the *Xba*I and *BglII* sites of pGEX-8P. A universal GUS-GFP expression plasmid pTUE-GFP3 was used for the scoring analysis for NLS activity in yeast. pTUE-GFP3 encodes the enhanced GFP fused with bacterial β-glucuronidase (GUS) under the control of a Tet operator-containing promoter and chimeric terminator in a vector derived from pGAD424 (Clontech; Palo Alto, CA). The GFP fused with the GUS protein brought about the cytoplasmic localization of the fusion protein, enabling a more sensitive assay than the native GFP protein. A Tet activator expression plasmid pGBKT-tTA was generated by cloning the coding region of tTA from pTet-Off (Clontech) into the *Xho*I and *BamHI* sites of a derivative of pGBKT7 (Clontech). A yeast-specific GFP expression plasmid pGAD-GFP was generated by replacement of the *Hind*III fragment of pGAD424 with a fragment containing the GFP-MCS region derived from pCMV-GFP2. A low-copy plasmid pAUA-GFP was derived from pAUR112 (Takara; Shiga, Japan) and contained the GFP-MCS region under the control of the *adh1* promoter. Double-stranded oligonucleotides encoding bimax1 and bimax2 were inserted into the *Xba*I and *BamHI* sites of pGAD-GFP and pAUA-GFP, and the resulting constructs were used for a yeast viability test. For an inducible expression plasmid pYES-GFP3, a *SmaI* fragment containing the Tet operator-minimal promoter region of pTUE-GFP3 was replaced with the *GAL1* promoter fragment of pYES-Trp2 (Invitrogen; Tokyo, Japan). Another inducible plasmid pYES-Grx1 was generated by inserting a PCR-amplified yeast genomic fragment that encode-Grx1p (a glutaredoxin with a molecular weight of approximately 12 kDa) into the *Pvu*II site of pYES-Trp2. A double-stranded oligonucleotide encoding a FLAG tag was inserted into the *BamHI* and *Sac*I sites of pYES-Grx1 to generate pYES-Grx1-FLAG. DNA fragments encoding NLSs (SV40, BPSV40, bimax1, and bimax2) were inserted into the *Xba*I and *BamHI* sites of pYES-GFP3 and the *Nhe*I and *BamHI* sites of pYES-Grx1 or pYES-Grx1-FLAG. An Nab2 NLS, which corresponded to a 50 aa region (residues 200–249) of the yeast Nab2p (a poly(A) RNA binding protein), was PCR amplified with a primer set (Nab2-N and Nab2-C) and inserted into pYES-GFP3. A mammalian GFP expression plasmid pCMV-GFP2 was generated by replacement of a MCS located at the 3′ end of the GFP coding region of pQBI25-fC1 with another one containing *Xba*I and *BamHI* sites. A plasmid pCMV-GFP3 for expression of a GUS-GFP fusion protein was generated by inserting the GUS coding fragment into the *Nhe*I site located at the 5′ end of the GFP coding sequence of pCMV-GFP2. For an expression plasmid pCMV-Grx1 used for a competitor NLS expression, the Grx1 coding fragment was inserted into the *Nhe*I and *BamHI* sites of pCMV-GFP2 to replace the GFP coding region. Double-stranded oligonucleotides encoding NLS peptides or cDNA fragments were inserted into the *Xba*I and *BamHI* sites of these plasmids. The cDNA fragments encoding Snail, PIASy, EZI, and the N-terminal region (residues 1–481) of SREBP-2 were PCR amplified with oligo(dT)-primed first-strand cDNAs from human as template, and cDNAs of hnRNP-A1 and p107 were PCR-amplified with first-strand cDNAs from mouse using specific primers (Table S1).

Systematic Amino Acid Replacement Analysis

Double-stranded oligonucleotides encoding NLS variants were inserted into the *Xba*I and *BamHI* sites of pTUE-GFP3. We used double-stranded oligonucleotides containing NN(G/C) at a position of an amino acid residue to be replaced (biNC-m1 and cbiNC-m1 as an example of oligonucleotides; see Table S1). Plasmid clones encoding NLSs containing 13–19 different amino acids at each position within an NLS template were routinely selected from 48 randomly selected bacterial colonies. The selected plasmids were introduced into yeast, and the extents of the nuclear localization of the expressed GUS-GFP-NLS fusion proteins were assayed in yeast.

Yeast Transformation, Mammalian Cell Transfection

SFY526 yeast strain (Clontech) was cotransformed with 0.5 μg each of pTUE-GFP3 and pGBK-tTA, and cultured with SD medium lacking leucine and tryptophan in 48-well plates at 30°C. Alternatively, yeast was transformed with 0.5 μg of pGAD-GFP or pAUA-GFP and cultured with SD medium lacking leucine or uracil. The yeast expressing tTA grew very slowly, and so the transformed cells were cultured for at least 3 days. For the *GAL1* promoter-driven constructs, yeast was cotransformed with 0.5 μg each of a GFP reporter (pYES-GFP3) and a competitor NLS expression plasmid (pYES-Grx1), and the cells grown in SD medium lacking leucine and tryptophan were transferred to YPD medium containing 0.1% galactose instead of 2% glucose and grown for 2–3 hr. *KAP60-GFP* strain was constructed by transformation with a PCR fragment amplified with a primer set (Kap-GFP and Leu2-Kap) and using the pGAD-GFP plasmid as template. The amplified fragment comprised a hemagglutinin tag (HA)-*GFP-Tadh1-Leu2* gene cassette flanked by 44 bp of homology regions of *KAP60* to allow in-flame fusion with the HA-GFP tag at the C-terminal coding region of *Kap60p*. Strain YNN141 (*MATa his3-532 trp1-289 ura3-1 ura3-2 ade2 leu2::HIS3*), a derivative of YNN140 (National Institute of Technology and Evaluation, Biological Resource Center, Kisarazu, Chiba, Japan) was transformed with the PCR fragment and a strain was selected with SD medium lacking leucine. The correct insertion into the yeast chromosome was verified by PCR followed by sequencing. The mouse fibroblast cell line NIH 3T3 was grown at 37°C under 5% CO_2 in DMEM supplemented with 10% calf serum and 2 mM l-glutamine. Transfections were performed in 5×10^4 cells per milliliter in 24-well plates or 35 mm culture dishes, and the cells were cotransfected with approximately 0.4 μg of a GFP reporter plasmid and 0.4 μg of a competitor expression plasmid (pCMV-Grx1) using 2 μl of jet-PEI reagent (Polyplus-transfection; Strasbourg, France) according to the manufacturer's instructions and -cultured for 36–48 hr. GFP expressed in these transformed cells was observed using an epifluorescence microscope, model BX51 (Olympus; Tokyo, Japan), with an excitation filter specific to 460–490 nm.

Production of Recombinant Proteins

Proteins fused with glutathione S-transferase (GST) were expressed in *E. coli* BL21 by induction with 0.6 mM isopropyl-beta-D-thiogalactopyranoside (IPTG) followed by sequential incubation each for 2 hr at 37°C and 30°C. The harvested bacterial pellets were resuspended with extraction buffer (20 mM HEPES-NaOH [pH 7.5], 0.5 M NaCl, 10 mM EDTA, 0.1% Triton X-100, and 5% protease inhibitor cocktail [Sigma-Aldrich]), lysed by sonication, and cleared by centrifugation. The supernatants were loaded onto columns containing glutathione sepharose 4B (Amersham Biosciences), and the columns were washed with washing buffer (20 mM HEPES NaOH [pH 7.5], 0.15 M NaCl, and 1 mM EDTA) and eluted with the washing buffer containing 10 mM glutathione. Trx-GFP proteins fused with various NLS sequences were expressed in BL21(DE3) by induction with 1 mM IPTG followed by sequential incubation each for 2 hr at 37°C and 30°C, and purified with Ni-NTA His-Bind resin (Novagen) under native conditions, according to the manufacturer's instructions. The purified proteins were dialyzed with the washing buffer.

Importin Binding Assay

The purified GST-importin fusion protein was incubated with a Trx-GFP-NLS protein in 20 μl of reaction buffer (20 mM HEPES-NaOH [pH 7.4], 0.1 M NaCl, 1 mM DTT, 1 mM EDTA, 5 mM $MgCl_2$, 10% glycerol, and 0.1% BSA) for 60 min at room temperature. The reactions were electrophoresed on native 7.5% polyacrylamide gel/1 × Tris-glycine buffer containing 1 mM DTT and 10% glycerol for 50 min under a constant voltage of 160 V. The GFP fluorescence of Trx-GFP fusion proteins on the gel was observed with a fluorescence image analyzer, Molecular Imager FX (Bio-Rad Japan; Tokyo, Japan).

Surface Plasmon Resonance Analysis

Surface plasmon resonance (SPR) experiments were performed using a Biacore 3000 system (GE Healthcare; Tokyo, Japan). All experiments were carried out at 25°C at a flow rate of 10 μl min^{-1} in HBS running buffer (10 mM HEPES [pH 7.4], 150 mM NaCl, 0.005% surfactant P20). CM5 sensor chip surfaces were activated by using a thiol coupling kit (GE Healthcare). NLS peptide variants fused with Trx-GFP were immobilized to the activated surfaces by thiol coupling via cysteine residues of the Trx-GFP protein at a density of 500–1000 resonance units (RU). Various concentrations of analytes (GST-Kap60p and GST-Kap60pΔIBB) were injected into flow cells of the sensor chips to obtain SPR sensorgrams for the interaction of the peptides with the importin α variants. After each injection, the chip surfaces were regenerated with 5 or 10 μl of 10 mM NaOH. RUs of reference cells to which Trx-GFP alone was immobilized were subtracted from RUs of the peptide sensorgrams, but bulklike effects probably due to a weak interaction were still observed in several sensorgrams. Thus, for the curve-fitting analysis, we did not consider RUs obtained for a period of 10 s after the start and the end of analyte injection, respectively. The sensorgrams were analyzed by nonlinear regression, local fitting (each sensorgram separately) to 1:1 Langmuir model using BIAevaluation 3.1 software to determine the association and dissociation rate constants (k_{on} and k_{off}) and the dissociation equilibrium constants ($K_d = k_{off}/k_{on}$).

Immunoprecipitation

A 50 ml culture of exponentially growing yeast cells was induced with galactose for 3 hr and collected by centrifugation. The collected cells were lysed with glass beads and an extraction buffer (20 mM HEPES-NaOH [pH 7.5], 0.1 M NaCl, 5 mM $MgCl_2$, 5 mM EDTA, 5% glycerol, 0.5% Triton X-100, and protease inhibitor cocktail [Roche; Tokyo, Japan]). Lysates were incubated with anti-FLAG M2 agarose (Sigma-Aldrich Japan; Tokyo, Japan) for 2 hr at 4°C, and the beads washed four times with extraction buffer. Proteins bound to the beads were eluted with 0.1 M glycine (pH 3.5) and the eluates mixed with Laemmli sample buffer. One-tenth aliquots of the samples were subjected to western blotting with anti-FLAG M2 and anti-HA monoclonal antibodies (Sigma), and the blots developed by using a western blue stained substrate for alkaline phosphatase (Promega; Tokyo, Japan).

SUPPLEMENTAL DATA

Supplemental Data include three figures and one table and can be found with this article online at http://www.chembiol.com/cgi/content/full/15/9/940/DC1/.

ACKNOWLEDGMENTS

We thank Nobutaka Matsumura for advising us on a GFP localization analysis in mammalian cells. This work was supported by grants from Yamagata prefectural government and Tsuruoka City.

Received: February 20, 2008
Revised: July 7, 2008
Accepted: July 21, 2008
Published: September 19, 2008

REFERENCES

Arnold, M., Nath, A., Wohlwend, D., and Kehlenbach, R.H. (2006). Transportin is a major nuclear import receptor for c-Fos: a novel mode of cargo interaction. J. Biol. Chem. *281*, 5492–5499.

Cansizoglu, A.E., Lee, B.J., Zhang, Z.C., Fontoura, B.M., and Chook, Y.M. (2007). Structure-based design of a pathway-specific nuclear import inhibitor. Nat. Struct. Mol. Biol. *14*, 452–454.

Conti, E., Uy, M., Leighton, L., Blobel, G., and Kuriyan, J. (1998). Crystallographic analysis of the recognition of a nuclear localization signal by the nuclear import factor karyopherin α. Cell *94*, 193–204.

Fagerlund, R., Kinnunen, L., Köhler, M., Julkunen, I., and Melén, K. (2005). NF-κB is transported into the nucleus by importin α3 and importin α4. J. Biol. Chem. *280*, 15942–15951.

Forwood, J.K., Lam, M.H., and Jans, D.A. (2001). Nuclear import of Creb and AP-1 transcription factors requires importin-β 1 and Ran but is independent of importin-α. Biochemistry *40*, 5208–5217.

Fox, R.J., Davis, S.C., Mundorff, E.C., Newman, L.M., Gavrilovic, V., Ma, S.K., Chung, L.M., Ching, C., Tam, S., Muley, S., et al. (2007). Improving catalytic function by ProSAR-driven enzyme evolution. Nat. Biotechnol. *25*, 338–344.

Gilchrist, D., Mykytka, B., and Rexach, M. (2002). Accelerating the rate of disassembly of karyopherin.cargo complexes. J. Biol. Chem. *277*, 18161–18172.

Gilchrist, D., and Rexach, M. (2003). Molecular basis for the rapid dissociation of nuclear localization signals from karyopherin α in the nucleoplasm. J. Biol. Chem. *278*, 51937–51949.

Görlich, D., and Kutay, U. (1999). Transport between the cell nucleus and the cytoplasm. Annu. Rev. Cell Dev. Biol. *15*, 607–660.

Görlich, D., Prehn, S., Laskey, R.A., and Hartmann, E. (1994). Isolation of a protein that is essential for the first step of nuclear protein import. Cell *79*, 767–778.

Görlich, D., Vogel, F., Mills, A.D., Hartmann, E., and Laskey, R.A. (1995). Distinct functions for the two importin subunits in nuclear protein import. Nature *377*, 246–248.

Harel, A., and Forbes, D.J. (2004). Importin β: conducting a much larger cellular symphony. Mol. Cell *16*, 319–330.

Harreman, M.T., Hodel, M.R., Fanara, P., Hodel, A.E., and Corbett, A.H. (2003). The auto-inhibitory function of importin α is essential in vivo. J. Biol. Chem. *278*, 5854–5863.

Hodel, A.E., Harreman, M.T., Pulliam, K.F., Harben, M.E., Holmes, J.S., Hodel, M.R., Berland, K.M., and Corbett, A.H. (2006). Nuclear localization signal receptor affinity correlates with in vivo localization in *Saccharomyces cerevisiae*. J. Biol. Chem. *281*, 23545–23556.

Hodel, M.R., Corbett, A.H., and Hodel, A.E. (2001). Dissection of a nuclear localization signal. J. Biol. Chem. *276*, 1317–1325.

Hood, J.K., and Silver, P.A. (1998). Cse1p is required for export of Srp1p/importin-α from the nucleus in *Saccharomyces cerevisiae*. J. Biol. Chem. *273*, 35142–35146.

Hood, J.K., Casolari, J.M., and Silver, P.A. (2000). Nup2p is located on the nuclear side of the nuclear pore complex and coordinates Srp1p/importin-alpha export. J. Cell Sci. *113*, 1471–1480.

Jans, D.A., Xiao, C.Y., and Lam, M.H. (2000). Nuclear targeting signal recognition: a key control point in nuclear transport? Bioessays *22*, 532–544.

Ladbury, J.E., Lemmon, M.A., Zhou, M., Green, J., Botfield, M.C., and Schlessinger, J. (1995). Measurement of the binding of tyrosyl phosphopeptides to SH2 domains: a reappraisal. Proc. Natl. Acad. Sci. USA *92*, 3199–3203.

Lange, A., Mills, R.E., Lange, C.J., Stewart, M., Devine, S.E., and Corbett, A.H. (2007). Classical nuclear localization signals: definition, function, and interaction with importin α. J. Biol. Chem. *282*, 5101–5105.

Lin, Y.Z., Yao, S.Y., Veach, R.A., Torgerson, T.R., and Hawiger, J. (1995). Inhibition of nuclear translocation of transcription factor NF-κ B by a synthetic peptide containing a cell membrane-permeable motif and nuclear localization sequence. J. Biol. Chem. *270*, 14255–14258.

Mildvan, A.S. (2004). Inverse thinking about double mutants of enzymes. Biochemistry *43*, 14517–14520.

Miyamoto, Y., Hieda, M., Harreman, M.T., Fukumoto, M., Saiwaki, T., Hodel, A.E., Corbett, A.H., and Yoneda, Y. (2002). Importin α can migrate into the nucleus in an importin β- and Ran-independent manner. EMBO J. *21*, 5833–5842.

Nagoshi, E., Imamoto, N., Sato, R., and Yoneda, Y. (1999). Nuclear import of sterol regulatory element-binding protein-2, a basic helix-loop-helix-leucine zipper (bHLH-Zip)-containing transcription factor, occurs through the direct interaction of importin β with HLH-Zip. Mol. Biol. Cell *10*, 2221–2233.

Neduva, V., and Russell, R.B. (2006). Peptides mediating interaction networks: new leads at last. Curr. Opin. Biotechnol. *17*, 465–471.

Pollard, V.W., Michael, W.M., Nakielny, S., Siomi, M.C., Wang, F., and Dreyfuss, G. (1996). A novel receptor-mediated nuclear protein import pathway. Cell *86*, 985–994.

Privé, G.G., and Melnick, A. (2006). Specific peptides for the therapeutic targeting of oncogenes. Curr. Opin. Genet. Dev. *16*, 71–77.

Robbins, J., Dilworth, S.M., Laskey, R.A., and Dingwall, C. (1991). Two interdependent basic domains in nucleoplasmin nuclear targeting sequence: identification of a class of bipartite nuclear targeting sequence. Cell *64*, 615–623.

Saijou, E., Itoh, T., Kim, K.W., Iemura, S., Natsume, T., and Miyajima, A. (2007). Nucleocytoplasmic shuttling of the zinc finger protein EZI Is mediated by importin-7-dependent nuclear import and CRM1-independent export mechanisms. J. Biol. Chem. *282*, 32327–32337.

Sandberg, W.S., and Terwilliger, T.C. (1993). Engineering multiple properties of a protein by combinatorial mutagenesis. Proc. Natl. Acad. Sci. U.S.A. *90*, 8367–8371.

Sato, A.K., Viswanathan, M., Kent, R.B., and Wood, C.R. (2006). Therapeutic peptides: technological advances driving peptides into development. Curr. Opin. Biotechnol. *17*, 638–642.

Schlenstedt, G., Hurt, E., Doye, V., and Silver, P.A. (1993). Reconstitution of nuclear protein transport with semi-intact yeast cells. J. Cell Biol. *123*, 785–798.

Sekimoto, T., Imamoto, N., Nakajima, K., Hirano, T., and Yoneda, Y. (1997). Extracellular signal-dependent nuclear import of Stat1 is mediated by nuclear pore-targeting complex formation with NPI-1, but not Rch1. EMBO J. *16*, 7067–7077.

Siomi, M.C., Fromont, M., Rain, J.C., Wan, L., Wang, F., Legrain, P., and Dreyfuss, G. (1998). Functional conservation of the transportin nuclear import pathway in divergent organisms. Mol. Cell. Biol. *18*, 4141–4148.

Solsbacher, J., Maurer, P., Vogel, F., and Schlenstedt, G. (2000). Nup2p, a yeast nucleoporin, functions in bidirectional transport of importin α. Mol. Cell. Biol. *20*, 8468–8479.

Torgerson, T.R., Colosia, A.D., Donahue, J.P., Lin, Y.Z., and Hawiger, J. (1998). Regulation of NF-kappa B, AP-1, NFAT, and STAT1 nuclear import in T lymphocytes by noninvasive delivery of peptide carrying the nuclear localization sequence of NF-κ B p50. J. Immunol. *161*, 6084–6092.

Truant, R., Fridell, R.A., Benson, R.E., Bogerd, H., and Cullen, B.R. (1998). Identification and functional characterization of a novel nuclear localization signal present in the yeast Nab2 poly(A)+ RNA binding protein. Mol. Cell. Biol. *18*, 1449–1458.

Vargo, M.A., Nguyen, L., and Colman, R.F. (2004). Subunit interface residues of glutathione S-transferase A1–1 that are important in the monomer-dimer equilibrium. Biochemistry *43*, 3327–3335.

Waldmann, I., Walde, S., and Kehlenbach, R.H. (2007). Nuclear import of c-Jun is mediated by multiple transport receptors. J. Biol. Chem. *282*, 27685–27692.

Weis, K. (2003). Regulating access to the genome: nucleocytoplasmic transport throughout the cell cycle. Cell *112*, 441–451.

Wells, J.A. (1990). Additivity of mutational effects in proteins. Biochemistry *29*, 8509–8517.

Wells, J.A., and McClendon, C.L. (2007). Reaching for high-hanging fruit in drug discovery at protein-protein interfaces. Nature *450*, 1001–1009.

Yamasaki, H., Sekimoto, T., Ohkubo, T., Douchi, T., Nagata, Y., Ozawa, M., and Yoneda, Y. (2005). Zinc finger domain of Snail functions as a nuclear localization signal for importin β-mediated nuclear import pathway. Genes Cells *10*, 455–464.

Yashiroda, Y., and Yoshida, M. (2003). Nucleo-cytoplasmic transport of proteins as a target for therapeutic drugs. Curr. Med. Chem. *10*, 741–748.